THE JOURNAL OF PHYSICAL CHEMISTRY Letters

Perspective

Cite This: J. Phys. Chem. Lett. 2018, 9, 6853−6863

pubs.acs.org/JPCL

How Lattice Dynamics Moderate the Electronic Properties of Metal-Halide Perovskites

Laura M. Herz*

Department of Physics, University of Oxford, Clarendon Laboratory, Parks Road, Oxford OX1 3PU, U.K.

ABSTRACT: Metal-halide perovskites have emerged as highly promising semiconductors with excellent optoelectronic properties. This Perspective outlines how the dynamic response of the ionic lattice affects key electronic properties such as exciton binding energies and charge-carrier mobilities in hybrid perovskites. Such links are shown to derive from the frequency-dependence of the dielectric function, which is governed by contributions from electronic interband transitions, polar vibrations of the metal-halide sublattice, organic cation collective reorientations, and ionic movement. The influence of each of these contributions to charge-carrier screening and carrier−lattice interactions is discussed, which allows for general trends with material composition to be revealed. Overall, this Perspective highlights the challenges and questions arising from the peculiar combination of a soft polar metal-halide sublattice interspersed with rotationally mobile dipolar molecules that is encountered in hybrid metal-halide perovskites.

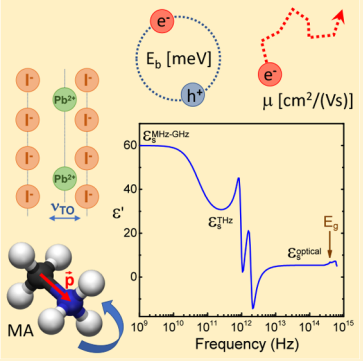

Metal-halide perovskites have proven to be a fascinating class of semiconductors, offering excellent optoelectronic properties[1,2] that have underpinned the superior performance of photovoltaic devices based on these materials.[3] An understanding of how the stoichiometry and structure of such perovskites affects their basic electronic properties will be essential for future advances in performance. Currently, the precise mechanisms determining fundamental electronic properties, such as exciton binding energies, charge-carrier mobilities, and recombination are still under scrutiny. These properties are strongly influenced by the lattice, which interacts directly with charge carriers but also moderates the interaction between electrons and holes through dielectric screening. Therefore, an examination of the dynamic response of the lattice and its effect on the dielectric environment is a necessary step toward a fuller understanding of the electronic properties of any semiconductor.

For hybrid metal-halide perovskites of ABX_3 stoichiometry, such investigations are particularly intriguing, because these materials exhibit a complex vibrational space that stretches over a vast frequency range. While organic A-cations may leave a vibrational footprint in the infrared part of the spectrum that arises from internal molecular vibrations,[4−9] the polar (optical) modes of the metal-halide sublattice are found at much lower THz frequencies.[5,8−12] In the 100 GHz range, collective reorientations of the A-cation may onset,[13−17] while at very low frequencies ($<10^4$ Hz), slow motion of ions through the lattice commence.[15,18,19]

The dynamic response of the lattice directly contributes to the dielectric environment experienced by charge carriers in metal-halide perovskites. For example, the Coulombic attraction between electrons and holes that is responsible for bound excitonic states may be screened by suitable lattice polarizabilities. In addition, the coupling of charge carriers to the electric fields arising from lattice dynamics can slow the motion of carriers, which limits attainable mobilities. However, the extent to which particular lattice dynamics and vibrations influence exciton binding energies and charge-carrier mobilities is still a matter of intense discussion. This Perspective reflects on the current state of the field, analyzing experimental and theoretical findings in order to unravel the interplay between the dielectric response of metal-halide perovskites and their fundamental electronic properties, such as exciton binding energies and charge-carrier mobilities.

The dynamic response of the lattice directly contributes to the dielectric environment experienced by charge carriers in metal-halide perovskites.

Dielectric Function. Figure 1 shows a schematic diagram of the frequency-dependent relative permittivity (real part) of $MAPbI_3$ at room temperature, derived from averages over a number of literature reports covering a range of frequency intervals.[4,10,11,15−30] Viewed from the high-frequency end ($>10^{15}$ Hz) downward, the dielectric function progressively rises with each resonance that is encountered toward lower frequency. Every process contributing to the dielectric response generates a sharp feature centered at its resonance frequency, with the contribution falling off to a nonzero static contribution toward lower frequency, as expected from the simple Drude−Lorentz model of a damped harmonic oscillator driven by an oscillating electric field.[31] Toward lower

Received: September 12, 2018
Accepted: November 13, 2018
Published: November 13, 2018

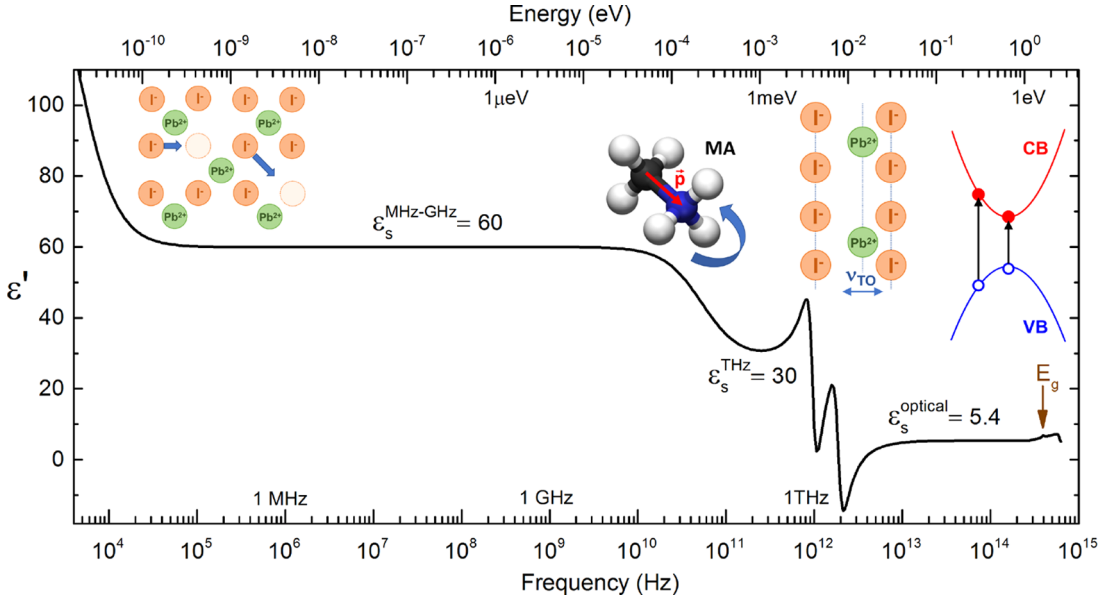

Figure 1. Schematic representation of the frequency-dependent relative permittivity (real part) of $MAPbI_3$ at room temperature, derived from averages over a number of literature reports covering various different frequency intervals.[4,10,11,15−30] Features around 4−8 × 10^{14} Hz are associated with electronic interband transitions; strong resonances near 1 and 2 THz derive from optical phonon resonances of the lead-iodide lattice. An increase in dielectric response near 100 GHz is associated with collective reorientation of MA cations. The rise in the value of ϵ' toward the low-frequency (≤10^4 Hz) regime originates from slow migration of ions, in particular, iodide.

frequencies, each subsequent electronic response therefore contributes an additional background offset to the overall value of the dielectric function. Figure 1 illustrates the four main contributors to the overall polarization response in $MAPbI_3$, which are electronic interband transitions, polar vibrations of the lead-iodide sublattice, MA cation collective reorientations, and ionic movement.

At the high-frequency end, electronic transitions across the band gap of $MAPbI_3$ ($E_g \approx 1.6$ eV; $\lambda_g \approx 770$ nm; $\nu_g \approx 3.9 \times 10^{14}$ Hz) create sharp absorption onsets linked to resonance features in the dielectric function, according to Kramers−Kroenig relations.[21,25] Such optical transitions are followed by a quasi-static response, $\epsilon_s^{optical}$, in the near-IR frequency range, whose value is evaluated here from a statistical average over 12 experimental literature reports[4,18,20−23,25−30] as $\epsilon_s^{optical} = 5.4 \pm 0.6$. Intramolecular vibrations associated with chemical bonds of MA cations leave signatures in the IR spectrum, but these only make relatively minor contributions to the dielectric response.[4,5]

Toward lower frequencies, polar vibrations (optical phonons) of the lead-halide sublattice are subsequently encountered, with resonances around 1−2 THz.[5,8−12] At their respective low-frequency end, these resonances result in a quasi-static value of the dielectric function of $\epsilon_s^{THz} = 30.4 \pm 6$, as calculated from an average over four reported measurements in the THz−GHz regime.[10,11,20,24]

In the region around and just below 100 GHz, collective rotational motion of the MA cation and its associated dipole moment along the C−N bond axis contribute.[13−16,24,32−39] Knowledge of the exact frequency-dependence of the dielectric function near the onset of these molecular reorientations is still relatively sparse, but recent experiments suggest an approximate onset near 200 GHz,[15] in agreement with reports of picosecond reorientation times of MA in $MAPbI_3$.[13,14,24,32,37−39] Such collective MA−dipole polarization lifts the background value of the dielectric function appreciably toward the GHz−MHz regime, yielding values of $\epsilon_s^{MHz-GHz} = 60 \pm 14$, according to an average over five experimental reports.[15−19]

Toward the low-frequency end, further increases in the apparent dielectric function near 1−10 kHz have commonly been reported.[15,18,19] These rises can be substantial in their magnitude and may be enhanced under illumination.[19] They are now generally attributed to slow ionic migration,[40] in particular of I^-, which has a relatively low energetic hurdle to motion in $MAPbI_3$.[41]

Exciton Binding Energies. Polarization responses such as those described above play a major role in mediating the screening of Coulombic interactions between electrons and holes in a semiconductor.[31,42] For metal hybrid perovskites, the resulting magnitude of the exciton binding energy E_b has been the subject of much discussion over the past few years.[2] Values of E_b below thermal energies at room temperature (26 meV) are highly desirable, because bound electron−hole states (excitons) need to be dissociated in order to contribute to the photocurrent of a photovoltaic device. The dependence of the exciton binding energy on electronic polarizability is captured in the hydrogenic model of the Wannier exciton, for which the exciton binding energy is given by[2,31]

$$E_b = Ry \frac{1}{\epsilon^2} \frac{m_r^*}{m_e} \quad (1)$$

where Ry = 13.606 eV is the Rydberg constant and m_r^*/m_e is the reduced effective mass of the electron−hole system (~0.10 for $MAPbI_3$[43]), expressed as a fraction of the free electron mass m_e. As discussed above, the permittivity ϵ entering eq 1 is a particularly strong function of frequency in lead-halide perovskites, which has opened a lively debate[2,18,43] on which value of ϵ ought to be chosen when E_b is evaluated through eq 1. In particular, a polarization response whose resonance energy falls significantly below E_b may not contribute effectively to screening, given that it then cannot fully follow

DOI: 10.1021/acs.jpclett.8b02811
J. Phys. Chem. Lett. 2018, 9, 6853−6863

the motion of the electron−hole pair.[42] Therefore, the question of which polarization contributes to exciton screening is intimately related to the frequency-dependence of the dielectric function.

To resolve this issue, one may contrast the dielectric response with values of exciton binding energies E_b (and the corresponding frequencies $\nu_b = E_b/h$) that have been determined independently of ϵ. Such direct assessments are offered through magneto-absorption studies,[43,44] or alternatively, an analysis of the shape of optical absorption onsets through Elliott's theory.[35,45−49] Taking averages over the values reported in these articles for the prototypical $MAPbI_3$, we find $E_b = 12 \pm 7$ meV at room temperature and $E_b = 23 \pm 7$ meV at low temperature (10 K), equivalent to frequencies $\nu_b = E_b/h$ of 2.9 and 5.6 THz, respectively. Hence, the origin of the dielectric response in the THz region of the spectrum requires particular scrutiny. Here, the low energies of the lead-iodide transverse optical phonon modes near $E_{Pb-I} = 4-8$ meV (1−2 THz),[5,12,20] caused by the heavy nature of lead, complicates the picture substantially. For exciton binding energies significantly below the optical phonon energies, ϵ_s^{THz} should enter eq 1, while the value of $\epsilon_s^{optical}$ is usually applied when E_b is appreciably larger.[42] The above considerations suggest that $MAPbI_3$ is an intermediate case, for which E_{Pb-I} falls relatively close to (or just below) E_b. For such a scenario, the Haken potential may be utilized to interpolate between ϵ_s^{THz} and $\epsilon_s^{optical}$.[42,50] An additional subject of ongoing debate[32,35,51] is the question of whether molecular reorientations of the MA cations contribute to screening of the Coulomb interactions. Figure 1 indicates that these polarizations may raise the value of the dielectric function substantially; however, their onset may potentially fall at too low a frequency to contribute significantly to dielectric screening of the exciton.[51] Several pieces of evidence may elucidate this particular issue, as detailed below.

First, an effective value of ϵ_{eff} may be derived from eq 1 for $MAPbI_3$ under knowledge of the exciton binding energy and the effective reduced mass of the electron−hole system. Taking $m_r^*/m_e = 0.10$ from magneto-absorption measurements[43,44] and the room-temperature average of $E_b = 12 \pm 7$ meV evaluated above, we calculate $\epsilon_{eff} = 11 \pm 4$. Comparison with the dielectric function sketched in Figure 1 shows that such a value of epsilon falls in between those encountered for the low- and high-frequency limits of the optical phonon resonance (i.e., $\epsilon_s^{THz} < \epsilon_{eff} < \epsilon_s^{optical}$). Crucially, this also matches the THz frequency range near $\nu_b = E_b/h$, or in other words, when a directly measured value of the exciton binding energy is converted into an expected value of the dielectric function according to eq 1, that value of ϵ_{eff} maps accurately onto that actually measured at that energy or frequency. Such experimentally based self-consistency considerations thus suggest that $MAPbI_3$ indeed falls into an intermediate regime, for which the polarizability from optical transitions is partly augmented by that arising from optical phonons. Substantial contributions from molecular cation reorientation to excitonic screening would, on the other hand, be hard to rationalize, given that they would lead to a scenario that is not self-consistent with respect to the dielectric function and exciton binding energy pertaining to a given frequency.

As a second consideration, the temperature-dependence of the exciton binding energy could help identification of the mechanisms contributing to screening, given that the relevant dielectric contributions should mirror such changes. An analysis of the onset of the absorption spectrum through Elliott's theory[52] is particularly convenient here, as it can yield a value of E_b at any given temperature by unravelling bound excitons from continuum electron−hole contributions (see Figure 2a). Such measurements have been repeatedly carried out[45−48] for $MAPbI_3$ and typically show a decline in E_b with increasing temperature from ∼20−30 meV near 10 K to ∼12 meV near room temperature, with a step-like change occurring over a narrow temperature range near the tetragonal-to-orthorhombic phase transition at 160 K.[45−48] Figure 2b,c displays an example of such trends, as reproduced from Ref 45.

Experimental and theoretical examinations suggest that the major contributors to exciton screening are inorganic (metal-halide) lattice and electronic interband polarizations.

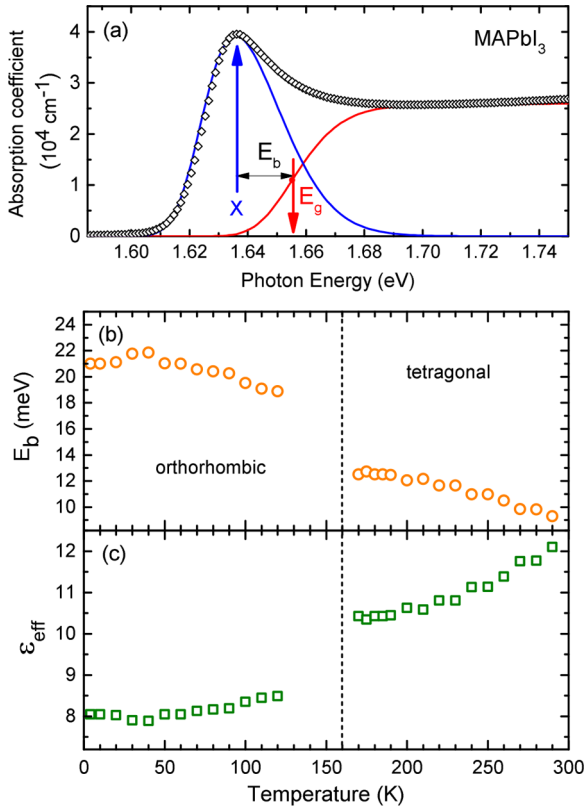

Figure 2. Figure illustrating the typical extraction of exciton binding energies in $MAPbI_3$ from modeling of the absorption onset with Elliott's theory (data taken from Ref 45 by Davies et al.). (a) Absorption onset (black open diamonds, experimental data) with fits from Elliott's theory, with the blue line showing the contribution from bound excitonic states and the red line that from continuum band-to-band transitions of free charge carriers. The difference between the lowest bound exciton transition energy (X) and the band gap (E_g) is the exciton binding energy E_b. (b) Exciton binding energy extracted from such fits, and (c) value of the dielectric function ϵ_{eff}, determined from eq 1 under the assumption of $m_r^*/m_e = 0.10$, plotted as a function of temperature (adopted from Ref 45). Note the discontinuity[45] in E_b and ϵ_{eff} near the orthorhombic-to-tetragonal phase transition[16] around 160 K.

DOI: 10.1021/acs.jpclett.8b02811
J. Phys. Chem. Lett. 2018, 9, 6853−6863

A broader survey across multiple literature studies[45−48] similarly reveals that E_b typically declines with increasing temperature by approximately 35% upon entry into the tetragonal phase, which corresponds to an increase by roughly 20% of the equivalent dielectric constant ϵ_{eff} relevant to excitonic screening (according to eq 1). Because the MA cation reorientation is frozen out in the low-temperature orthorhombic phase,[16,17,24,39] these changes have been viewed as evidence for a contribution of molecular dipole reorientation to excitonic screening upon entry into the tetragonal phase.[34,35] However, at the tetragonal-to-orthorhombic phase transition, variations in the electronic transitions (such as a change in band gap energy by 100 meV)[45,53] and the optical phonon modes (a splitting of peaks)[5,11,54] are also evident, which could potentially serve as markers for a modification of the polarizability associated with these resonances. Temperature-dependent measurements of optical absorption and refraction at near-IR ($\epsilon_s^{optical}$) and low-THz (ϵ_s^{THz}) frequencies[11,26,45] for $MAPbI_3$ show small changes in magnitude with temperature but clear modifications nearer the optical phonon resonances. More detailed measurements and analysis would be needed to understand whether the alterations observed in the optical phonon resonances at the phase transition could sufficiently affect exciton binding energies. Changes in the quasi-static value of the dielectric function at MHz and GHz frequencies with temperature, on the other hand, are clearly massive, with studies suggesting a 300% increase in the value of the dielectric function at 1 MHz[15,17] and 1 kHz[16] upon entry into the tetragonal phase when cation rotations are activated. However, at higher frequencies nearer 90 GHz, such effects already appear to be considerably weaker (≤10%),[24] suggesting that they do not penetrate significantly into the frequency range pertaining to exciton screening. To disentangle such effects more clearly, additional, detailed measurements of the temperature-dependence of the dielectric function in the GHz to THz region would help to support the ongoing debate. Such investigations may allow for a clearer differentiation between small changes of electronic and metal-halide lattice polarizations that strongly contribute to exciton screening, and large polarizability changes arising from molecular cation reorientation that are however less effective because they operate at much lower frequencies.

As a third consideration, the effect of A-cation or B-metal substitutions in ABX_3 perovskites could help to unravel the competing mechanisms that underpin exciton screening. Here, a particularly interesting comparison is between lead and tin perovskites (B = Pb^{2+} or Sn^{2+}), because incorporation of the lighter element Sn should lead to an upshift of the optical phonon frequencies ($\nu_{Sn-I} > \nu_{Pb-I}$) of the lattice, which may cause $\nu_b = E_b/h$ to fall at frequencies below ν_{Sn-I}. As a result, excitons in $ASnI_3$ perovskites are expected to experience more effective screening by the ionic metal-halide lattice, and one would expect exciton binding energies to be lower than those encountered in lead-based counterparts.[51,55] Recently, an exciton binding energy of only 3.1 meV in $FASnI_3$ has indeed been determined at 5 K through direct observation of interexcitonic transitions in the THz-frequency range,[56] which is lower than the typical values reported for lead-iodide perovskites. Such comparisons hence confirm the substantial contribution the ionic metal-halide lattice can make toward excitonic screening in metal-halide perovskites.

Comparison of exciton binding energies between perovskites containing a variety of A-cations, for example, $MAPbI_3$ and $FAPbI_3$, however appears to raise more complex issues. Such examinations could potentially elucidate the importance of molecular contributions to screening, given that MA and FA have different molecular dipole moments,[34] and their motion is curtailed differently when temperatures are lowered and the material undertakes structural phase transitions.[39,54] Experimental comparisons of directly measured values of E_b in $MAPbI_3$ and $FAPbI_3$ are still conflicting. While extrapolations from low-temperature magneto-absorption measurements found little change with A-cation substitution,[43] direct observations of interexcitonic resonances in the THz regime[54] have suggested that E_b is noticeably lower in $FAPbI_3$. Either way, one has to be cautious about interpreting even a substantial change in E_b with A-cation substitution as evidence for molecular cation reorientation contributing to Coulombic screening. Polar A-cations such as MA and FA are prone to forming hydrogen bonds with the inorganic metal-halide sublattice, which can alter the covalent/ionic character of the metal-halide bonds.[57] Direct couplings between the vibrational modes of the inorganic lead-iodide sublattice and the N−H stretch of FA and MA cations have indeed just been observed.[58] Therefore, changes in E_b with A-cation substitution may well be an indirect effect, deriving from the influence of the A-cation on the inorganic lead-halide sublattice, rather than from a direct contribution of organic A-cation rotation to screening.[59]

Tin-based perovskites have higher optical phonon frequencies such that the inorganic lattice may contribute more fully to screening, while the presence of heavy lead leads to an intermediate case, in which the inorganic lattice screens the exciton less effectively.

As a fourth approach, theoretical calculations may allow for a direct comparison of the different contributions to excitonic screening, including electronic, inorganic lattice, and molecular polarizabilities.[51,55,60,61] Unfortunately, a correct evaluation of the exciton binding energy from first principles poses a formidable challenge, because it requires the comparison of electronic transition energies obtained in the presence and absence of electron−hole interactions. In addition, the heavy nature of lead results in sizable spin−orbit coupling in $MAPbI_3$, requiring fully relativistic calculations for an accurate determination of electronic transition energies. Calculations to date have been based on the GW approach, which combines single-body Green's functions with the screened Coulomb interaction to yield the uncorrelated electron−hole transitions.[51,55,60,61] These absorption spectra are then compared with the solutions to the Bethe−Salpeter equation (BSE), which provides Coulomb-correlated excitonic states. The exciton binding energy is evaluated from the difference between the lowest transitions in the respective GW and BSE spectra.[51,55,60,61] Given that these onset energies are relatively large (~1.6 eV for $MAPbI_3$) compared with the expected exciton binding energy (few tens of meV) the need for accuracy is particularly high for these first-principles

DOI: 10.1021/acs.jpclett.8b02811
J. Phys. Chem. Lett. 2018, 9, 6853−6863

calculations. It is therefore perhaps not too surprising that theoretical values reported for E_b have been fairly divergent, ranging from $E_b \approx 150$ meV[61] over intermediate values of 40–45 meV[55,60] down to 15 meV[51] for $MAPbI_3$. Here, the value most comparable to the experimental results (15 meV) was obtained through a self-consistent approach, in which theoretical dependencies of the exciton binding energy on the effective value of the dielectric function (and vice versa) were ensured to be in agreement[51] (similar to the above arguments based on experimental findings). Through this approach, the authors also assessed the influence of a tentative polarization response from collective MA rotations (peaked near 200 GHz), which they concluded to be insignificant compared with the contributions from the inorganic metal-halide lattice.[51]

In summary, the exciton binding energy in any metal-halide perovskite is closely linked with the frequency-dependence of the dielectric function. Experimental and theoretical examinations suggest that the major contributors to exciton screening are inorganic (metal-halide) lattice and electronic interband polarizations. The strength of the metal-halide lattice contribution is largely influenced by whether binding energies fall above or below optical phonon frequencies. Tin-based perovskites have higher optical phonon frequencies such that the inorganic lattice may contribute more fully to screening, while the presence of heavy lead leads to an intermediate case, in which the inorganic lattice screens the exciton less effectively. The influence of collective rotations of the molecular A-cation, on the other hand, are much more difficult to assess. While such polarizations fall into too low an energy range to overlap fully with the range equivalent to exciton binding energies, they carry a polarization response with substantial magnitude. In addition, indirect effects by which the A-cation modulates the polarization response of the inorganic sublattice could give rise to a complex interplay that will be challenging to disentangle. Temperature-dependent measurements of the dielectric function in the frequency range relevant to exciton binding energies, for a range of different metal-halide perovskites, would help to support investigations in this area. A better understanding of the vibrational contributions to polarizabilities in the critical frequency range between 10 GHz to 1 THz, coupled with further advances in theoretical modeling, should lead to a resolution of the ongoing controversies surrounding excitonic binding energies.

Charge-carrier Mobilities. Vibrations may have a substantial effect on the motion of charge carriers through electron–phonon coupling. For a range of different metal-halide perovskites, including $MAPbI_3$,[53,62−65] $MAPbBr_3$,[66] $FAPbI_3$,[54] and $FASnI_3$,[56] the charge-carrier mobility was reported to increase substantially as the temperature is lowered. These trends suggest that charge-carrier motion is already dominated by coupling to phonon modes whose occupancy falls with decreasing temperature. The past few years have therefore seen a lively debate on the exact mechanisms underpinning electron–phonon coupling in metal-halide perovskites.[1,67]

By symmetry,[68,69] the two most likely contributors to electron–phonon coupling in $MAPbI_3$ are acoustic-phonon deformation potential (ADP) scattering and Fröhlich interactions with longitudinal optical (LO) phonons. Here, ADP scattering involves low-energy (≤meV) acoustic phonons that cause a temporary perturbation of the lattice, which modulate the electronic bands, coupling electronic levels to lattice vibrations (phonons). Fröhlich interactions,[70−73] on the other hand, result when the macroscopic electric field generated by a longitudinal optical phonon interacts with charge carriers. A clean distinction between such effects was made both experimentally[12] and theoretically[74−78] for lead-iodide perovskites. An experimental investigation revealed that electron–phonon coupling was markedly reduced below the characteristic temperature corresponding to the energy of the effective LO phonon (11.5 meV),[5] in agreement with Fröhlich interactions being the dominant mechanisms at room temperature.[12] Contributions from acoustic phonons, on the other hand, were found to be negligible by comparison,[12] as would be expected for a polar ionic semiconductor.[70] Theoretical calculations further suggested that ADP scattering is relatively weak for $MAPbI_3$ and should result in charge-carrier mobilities of several thousand $cm^2/(Vs)$ at room temperature if it were the sole mechanism in operation,[74,75] in contrast with values <100 $cm^2/(Vs)$ experimentally encountered[1] at room temperature. Ab initio calculations based on Fröhlich coupling[76−78] suggest this to have the dominant effect at room temperature, and yield more realistic charge-carrier mobility values near 100 $cm^2(Vs)^{-1}$. Therefore, the emerging literature consensus is that at room temperature, charge-carrier mobilities in metal-halide perovskites are intrinsically mostly limited by interactions between charge carriers and the LO phonon of the polar metal-halide lattice.

Such considerations mean that upper limits to charge-carrier mobilities in metal-halide perovskites can be fairly readily obtained from knowledge of values of the dielectric function and LO phonon energies. Within the Fröhlich model,[73,79] the mobility μ of a charge carrier is antiproportional to the coupling constant $\alpha = \epsilon_{Fr}^{-1}(Ry/\hbar\omega_{LO})^{1/2}(m^*/m_e)^{1/2}$, where ω_{LO} is the LO phonon energy, Ry = 13.606 eV the Rydberg constant, and m^*/m_e is the effective mass m^* of the charge carrier given as a fraction of the free electron mass m_e. The parameter $\epsilon_{Fr}^{-1} = \epsilon_{\infty}^{-1} - \epsilon_{static}^{-1}$ is determined by the static and high-frequency limits of the dielectric function with respect to the LO phonon resonance, that is, by the definitions given above, $\epsilon_{static} = \epsilon_s^{THz}$ and $\epsilon_{\infty} = \epsilon_s^{optical}$. Using the average values of $\epsilon_s^{THz} = 30.4$ and $\epsilon_s^{optical} = 5.4$ determined for $MAPbI_3$, as discussed above, and taking $\hbar\omega_{LO} = 11.5$ meV[5,12] and $m^*/m_e = 0.2$ for the electron mass,[45,80,81] we obtain $\alpha = 2.34$ for an electron in $MAPbI_3$, which is substantially higher than the equivalent value for GaAs ($\alpha = 0.069$ as derived from parameters tabled in Ref 82). Therefore, the significantly higher electron mobility in GaAs (9400 $cm^2/V^{-1}s^{-1}$)[82] compared to $MAPbI_3$ (~100 $cm^2V^{-1}s^{-1}$)[1] can be understood in terms of the higher LO phonon frequency of GaAs (~35 meV[82] compared with ~11 meV[5,12] in $MAPbI_3$) and the weaker ionic screening by the polar lattice[20] within the Fröhlich model, in conjunction with the significantly lower effective electron mass.[82]

Despite clear success of the Fröhlich model for the case of metal-halide perovskites, one remaining inconsistency appears to be the observed temperature-dependence of the charge-carrier mobility μ.

DOI: 10.1021/acs.jpclett.8b02811
J. Phys. Chem. Lett. 2018, 9, 6853−6863

Variations of the charge-carrier mobility with perovskite composition have been explored across a wide parameter space, as summarized in Ref 1. Here, the Fröhlich coupling mechanism can explain the significant differences in charge-carrier mobility between tin- and lead-based perovskites given that within the Fröhlich approach,[73,79] the charge-carrier mobility decreases with increasing temperature T as a function of the dimensionless parameter $\beta=\hbar\omega_{LO}/k_BT$. As mentioned above, use of the lighter element tin will lead to an increase in LO phonon frequencies ω_{LO}, which scales such mobility curves to higher temperatures; thus at any given temperature, a higher mobility ought to be expected for perovskites composed of significantly lighter B-metals than lead. In contrast, Fröhlich interactions have been proposed to increase along the halide series from I to Br to Cl,[12,20] which in this case is mostly attributable to the increased ionicity of the lead-halide bond. Such an increase in electron−phonon coupling is in agreement with experimental data showing a reduction in charge-carrier mobility from lead-iodide to lead-bromide perovskites of similar morphologies.[83,84] In a recent study,[20] the above-mentioned input parameters (such as LO phonon energies and limits of the dielectric function) were extracted from infrared reflectivity data (Reststrahlen band) for various lead-halide perovskites, yielding a Fröhlich-limited charge-carrier mobility value near 200 $cm^2/(Vs)$ for $MAPbI_3$. Such models therefore not only reproduce qualitative changes with perovskite composition (B- or X-substitution) but also yield absolute values that come close to the highest mobility values experimentally observed at room temperature.[1]

Despite clear success of the Fröhlich model for the case of metal-halide perovskites, one remaining inconsistency appears to be the observed temperature-dependence of the charge-carrier mobility μ. For the most commonly studied $MAPbI_3$ perovskite, a power-law temperature-dependence of $\mu \propto T^m$ with exponent $m = -1.5$ has consistently been reported.[53,62−64] Yet in a recent study, Frost[78] suggested that the temperature-dependence expected within the Fröhlich model (beyond the Boltzmann approximation)[73,79] should follow $\mu \propto T^{-0.46}$ at temperatures above the optical phonon emission threshold. This discrepancy between the experimental findings and theoretical predictions has triggered a discussion about whether mechanisms additional to the Fröhlich interaction must be considered in order for a complete picture to be obtained.

Here, one recent suggestion[85] has been that lattice anharmonicity should be taken into account for metal-halide perovskites, given that they are mechanically relatively soft[86] and exhibit low-energy features in their Raman spectra, which have been attributed to anharmonic polar fluctuations.[87] Since the Fröhlich model is based on harmonic approximations, such anharmonic contributions could potentially give rise to modifications to the expected temperature-dependence and values of the charge-carrier mobility. While harmonic assumptions are generally used to approximate the presence of a retention potential for the constituent parts of a solid, they are obviously never strictly applicable to *any* material, given that Coulomb interactions tail off toward long distances (leading, e.g., to the observable effect that any solid can be divided). Therefore, the question of whether a lattice potential is "harmonic" or "anharmonic" is misleading, since no lattice potential can ever be fully be harmonic. Instead the exact magnitude of such anharmonic effects needs to be queried, for example through potentially observed deviations of experimental findings from theories based on such harmonic approximations and agreement with theories that take account of the true lattice potential.

It has also been proposed that the contribution of the organic cation to the polarizability (Figure 1) may further lower the charge-carrier mobility in hybrid metal-halide perovskites,[15,88] in analogy to the discussion on exciton binding energies described above. However, a comparison of literature values for charge-carrier mobilities of ABX_3 metal-halide perovskites with different A-cations[1] does not reveal any particular trends with A-cation polarizability. Charge-carrier mobilities at THz frequencies exhibit no measurable differences with A-cation choice, with $CsPbI_3$,[89] $MAPbI_3$,[1,10] and $FAPbI_3$[1,83] thin films all yielding values near 30 $cm^2/(Vs)$. Similarly, $APbBr_3$ was found to exhibit comparable long-range diffusion constants[90] for A = Cs, MA, and FA, and the performance of $CsPbBr_3$ in photovoltaic devices seemed to match the best standard then achieved in the field for $MAPbBr_3$.[91] Similarly, variations in charge-carrier mobility observed upon Cs substitution in thin films of the $Cs_yFA_{1-y}Pb(Br_{0.4}I_{0.6})_3$ series were found to be mostly correlated with material crystallinity that arise from changes in compliance with the Goldschmidt tolerance factor.[84] Therefore, the current evidence available in the field does not support the idea that the polarizability of the A-cation has any substantial effect on charge-carrier mobilities.

A much simpler explanation for the observed temperature dependencies is that the values of ϵ_s^{THz} and $\epsilon_s^{optical}$ entering the calculation of the Fröhlich interaction parameter α could themselves be temperature-dependent.[92] The theoretical study by Frost[78] (predicting $\mu \approx T^{-0.46}$) did not account for a potential temperature variation of these parameters as a first approximation. As the debate with regards to excitonic effects above has made clear, the exact temperature-dependence of the dielectric function in these frequency ranges are still under some debate; therefore, this scenario represents another viable explanation.

It is useful to remember that even for classic inorganic polar semiconductors, the charge-carrier mobility does not necessarily vary with temperature according to $T^{-0.5}$.

Finally, it is still not entirely clear to what extent a simple inspection of exponents derived from such power laws can really be used to pin down the exact mechanisms limiting charge-carrier mobilities in these materials. Data examined to date have been relatively noisy, and error bars have not always been provided, which could mask an underlying wider distribution of exponents that derives from extrinsic effects. For example, while exponents near $m = -1.5$ have been reported four times for $MAPbI_3$,[53,62−64] one additional recent study finds values between −2 and −2.8.[65] In contrast, for $FAPbI_3$, $m = -0.52$ has recently been reported,[54] closer to the value proposed by Frost[78] within the Fröhlich model.[73,79] Therefore, the discrepancy between the theoretically expected and experimentally determined temperature-dependence of the charge-carrier mobility for $MAPbI_3$ does not even necessarily appear to be a universal feature of lead-iodide perovskites.

DOI: 10.1021/acs.jpclett.8b02811
J. Phys. Chem. Lett. 2018, 9, 6853−6863

Davies et al. proposed that the differing behavior observed for $MAPbI_3$ and $FAPbI_3$ could have extrinsic effects, deriving from regions of different structural phase that have been observed in $MAPbI_3$,[93] which could represent barriers to charge-carrier motion and whose prevalence will depend on the material temperature. Therefore, the exponents recorded from such measurements may not always represent the intrinsic electron−phonon coupling alone.

In this context, it is useful to remember that even for classic inorganic polar semiconductors, such as GaAs,[95] InSb,[94] InAs,[96] and InP,[97] the charge-carrier mobility does not necessarily vary with $T^{-0.5}$, even though a dominance of the Fröhlich mechanism would be expected at high temperatures. Figure 3 illustrates examples for temperature-dependent

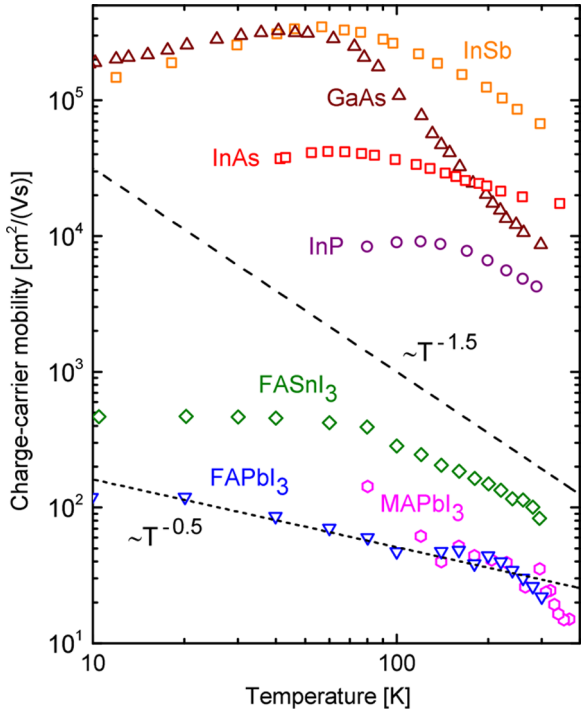

Figure 3. Charge-carrier mobility μ plotted as a function of temperature T for a range of semiconductors. Data for inorganic nonperovskite semiconductors are shown for n-type samples of doping density n_0, as determined from Hall measurements and taken from Refs 94 (InSb, orange squares, $n_0 = 9.8 \times 10^{14}$ cm^{-3}), 95 (GaAs, dark-red upward triangles, $n_0 = 2.5 \times 10^{13}$ cm^{-3}), 96 (InAs, red squares, $n_0 = 2 \times 10^{16}$ cm^{-3}) and 97 (InP, purple circles, $n_0 = 4.3 \times 10^{16}$ cm^{-3}). Data for thin films of hybrid metal-halide perovskites were taken from Refs 56 ($FASnI_3$, green diamonds, p-doped to $p_0 = 7.2 \times 10^{18}$ cm^{-3}), 54 ($FAPbI_3$, blue downward triangles), and 53 ($MAPbI_3$, pink hexagons) and had been recorded via optical-pump THz-probe spectroscopy; therefore, they represent the product of the charge-carrier mobility and the excitation-photon-to-free-charge branching ratio. The long-dashed line shows an illustrative temperature-dependence of $\mu \propto T^{-1.5}$, while the short-dashed line indicates $\mu \propto T^{-0.5}$.

carrier-mobilities of such semiconductors, taken from literature data,[94−97] together with those for $MAPbI_3$ (ref 53), $FAPbI_3$ (ref 54) and $FASnI_3$ (ref 56), presented on a double-logarithmic scale. The figure clearly highlights the phenomenal diversity of trends observed across the various polar semiconductors and over different sections of temperature. In particular, comparison with the dashed lines indicating different exponential dependencies indicate that very few of these data sets behave according to $\mu \approx T^{-0.5}$ over any significant temperature range. For polar inorganic semiconductors, it has long been known that a multitude of effects determines the exact temperature-dependence of the charge-carrier mobility, all of which have to be accounted for in order for the correct temperature-dependence to be reproduced.[98] The decreasing trend in mobility toward the lowest temperatures in particular has been attributed to scattering with shallow ionized impurities, which becomes more effective as the thermal velocity of charge carriers is slowed.[70,95,98] Similarly, it has recently been reported that the charge-carrier mobility increases substantially across all temperatures when $FASnI_3$ is passivated with SnF_2,[56] which reduces the prevalence of ionized defects arising from Sn vacancies.[99] Such treatments were also found to affect the exponent in the temperature-dependence of the mobility, with shallower rises toward low temperature being recorded for the highly p-doped material.[56] Therefore, a lingering contribution from ionized impurity scattering cannot necessarily be excluded for metal-halide perovskites, in particular, for tin-based perovskites that are prone to self-doping effects.[99−102]

Overall, the emerging picture suggests that charge-carrier mobilities in metal-halide perovskites are, as a first approximation, well captured within the Fröhlich model, which describes the coupling of charge carriers to the electric polarization field generated by the collective longitudinal vibrations of metal against halide ions. Absolute charge-carrier mobility values derived from this model appear to form reasonable upper limits when compared to the spread of available experimental data, and trends with compositional substitutions, e.g., along the halide series, or when swapping lead for tin, reproduce actual observations well. It is still an interesting open question to which extent additional effects, such as lattice anharmonicity and temperature-dependent ionic screening, need to be added for a more complete description of charge-carrier mobilities. Some care needs to be taken when temperature dependencies of the mobility are used to support arguments here, given that these trends may still be influenced by lingering extrinsic effects and multiple contributing mechanisms that have long been known from classic inorganic semiconductors, and which give rise to complex temperature dependencies.

It is still an interesting open question to which extent additional effects, such as lattice anharmonicity and temperature-dependent ionic screening, need to be added for a more complete description of charge-carrier mobilities.

Conclusions. The above considerations highlight that both exciton binding energies and charge-carrier mobilities in metal-halide perovskites sensitively depend on the frequency-dependence of the dielectric function. Polar metal-halide vibrations, in particular, have a significant impact on both exciton screening and charge-carrier mobilities. For lead-iodide perovskites, the heavy nature of lead yields optical phonon

DOI: 10.1021/acs.jpclett.8b02811
J. Phys. Chem. Lett. 2018, 9, 6853−6863

frequencies that are comparable to exciton binding energies, leading to an intermediate scenario, in which polar lattice screening is only partially experienced. For lighter tin ingredients, however, an upshift in optical phonon frequencies results in enhanced screening that supports lower exciton binding energies. Charge-carrier mobilities are, in the first instance, well described within the Fröhlich picture of coupling to polar metal-halide vibrations, yielding sensible upper limits of room-temperature values and trends with stoichiometry.

Any direct influence of collective rotations of the molecular A-cation, on the other hand, appears to be relatively marginal. For excitonic screening, self-consistency arguments centered around the value of the dielectric function suggest that collective A-cation reorientations fall into too low a frequency band to screen the Coulombic attraction between electrons and holes effectively. However, the research field needs to come to an understanding of how structural phase transitions in $MAPbI_3$ somewhat moderate exciton binding energies. Future studies that further investigate the coupling between organic cations and the lead-halide sublattice and additional investigations of the temperature-dependent dielectric response across a wide frequency range, may help to elucidate these issues. A move beyond the strong focus on the prototypical $MAPbI_3$ may also prove fruitful here, given that alternative perovskites such as $MAPbBr_3$[48] and $FAPbI_3$[54] have shown significantly weaker changes in interband transitions and exciton binding energies at their corresponding phase transitions. Similarly, there appears to be little experimental evidence for molecular cations influencing the charge-carrier mobility of hybrid metal-halide perovskites to any significant extent.

Secondary effects on charge-carrier mobilities, such as lattice anharmonicity and temperature-dependent ionic screening, are still currently under scrutiny. Here, the power-law temperature-dependence of the charge-carrier mobility in metal-halide perovskites has intensely been discussed and contrasted with theoretical model solutions. However, analogous investigations conducted on classic inorganic semiconductors decades ago suggest that one has to be cautious about drawing definite conclusions from modeling such trends with a single contributing mechanism. The wide variety of exponents reported for various metal-halide perovskites (and sometimes even for the same stoichiometry) indicates that multiple effects, some of which are linked to extrinsic parameters such as doping, may still be operational in some cases. In addition, room-temperature values of the charge-carrier mobilities recorded for most metal-halide perovskites are still somewhat below values expected from Fröhlich theory,[1] indicating lingering additional effects. Any comparison with theoretical models or simulations will therefore need to take account of the many minor and major overlapping contributions that can influence the charge-carrier mobility over various temperature ranges.

In summary, this Perspective highlights some of the fascinating challenges raised by the intriguing dielectric response of perovskites that comprise a soft, polar metal-halide sublattice of potentially heavy atomic ingredients, interspersed with organic dipolar molecules that exhibit temperature-dependent rotational freedoms. Discussions about the nature of the electronic properties of such peculiar systems will no doubt continue for some time to come.

AUTHOR INFORMATION

Corresponding Author

*E-mail: laura.herz@physics.ox.ac.uk.

ORCID

Laura M. Herz: 0000-0001-9621-334X

Notes

The author declares no competing financial interest.

Biography

Laura Herz is a Professor of Physics at the University of Oxford. She received her PhD in Physics from the University of Cambridge in 2002, was a Research Fellow at St. John's College Cambridge from 2001−2003 and moved to a faculty post at the University of Oxford in 2003. Her research interests lie in the area of organic, inorganic and hybrid semiconductors including aspects such as self-assembly, nanoscale effects, energy and charge transfer, and light harvesting for solar energy conversion.

ACKNOWLEDGMENTS

The author's research is financially supported by the Engineering and Physical Sciences Research Council UK.

REFERENCES

(1) Herz, L. M. Charge-Carrier Mobilities in Metal Halide Perovskites: Fundamental Mechanisms and Limits. *ACS Energy Lett.* **2017**, *2*, 1539−1548.

(2) Herz, L. M. Charge Carrier Dynamics in Organic-Inorganic Metal Halide Perovskites. *Annu. Rev. Phys. Chem.* **2016**, *67*, 65−89.

(3) Green, M. A.; Hishikawa, Y.; Dunlop, E. D.; Levi, D. H.; HohlEbinger, J.; HoBaillie, A. W. Solar Cell Efficiency Tables (Version 52). *Prog. Photovoltaics* **2018**, *26*, 427−436.

(4) Glaser, T.; Müller, C.; Sendner, M.; Krekeler, C.; Semonin, O. E.; Hull, T. D.; Yaffe, O.; Owen, J. S.; Kowalsky, W.; Pucci, A.; Lovrincic, R. Infrared Spectroscopic Study of Vibrational Modes in Methylammonium Lead Halide Perovskites. *J. Phys. Chem. Lett.* **2015**, *6*, 2913−2918.

(5) Perez-Osorio, M. A.; Milot, R. L.; Filip, M. R.; Patel, J. B.; Herz, L. M.; Johnston, M. B.; Giustino, F. Vibrational Properties of the Organic-Inorganic Halide Perovskite $CH_3NH_3PbI_3$ from Theory and Experiment: Factor Group Analysis, First-Principles Calculations, and Low-Temperature Infrared Spectra. *J. Phys. Chem. C* **2015**, *119*, 25703−25718.

(6) Pèrez-Osorio, M. A.; Lin, Q.; Phillips, R. T.; Milot, R. L.; Herz, L. M.; Johnston, M. B.; Giustino, F. Raman Spectrum of the Organic-Inorganic Halide Perovskite $CH_3NH_3PbI_3$ from First Principles and High-Resolution Low-Temperature Raman Measurements. *J. Phys. Chem. C* **2018**, *122*, 21703−21717.

(7) Patel, J. B.; Milot, R. L.; Wright, A. D.; Herz, L. M.; Johnston, M. B. Formation Dynamics of $CH_3NH_3PbI_3$ Perovskite Following Two-Step Layer Deposition. *J. Phys. Chem. Lett.* **2016**, *7*, 96−102.

(8) Ledinsky, M.; Löper, P.; Niesen, B.; Holovsky, J.; Moon, S.-J.; Yum, J.-H.; De Wolf, S.; Fejfar, A.; Ballif, C. Raman Spectroscopy of Organic-Inorganic Halide Perovskites. *J. Phys. Chem. Lett.* **2015**, *6*, 401−406.

(9) Quarti, C.; Grancini, G.; Mosconi, E.; Bruno, P.; Ball, J. M.; Lee, M. M.; Snaith, H. J.; Petrozza, A.; De Angelis, F. The Raman Spectrum of the $CH_3NH_3PbI_3$ Hybrid Perovskite: Interplay of Theory and Experiment. *J. Phys. Chem. Lett.* **2014**, *5*, 279−284.

(10) Wehrenfennig, C.; Liu, M.; Snaith, H. J.; Johnston, M. B.; Herz, L. M. Charge-Carrier Dynamics in Vapour-Deposited Films of the Organolead Halide Perovskite $CH_3NH_3PbI_{3-x}Cl_x$. *Energy Environ. Sci.* **2014**, *7*, 2269−2275.

(11) La-o-vorakiat, C.; Xia, H.; Kadro, J.; Salim, T.; Zhao, D.; Ahmed, T.; Lam, Y. M.; Zhu, J.-X.; Marcus, R. A.; Michel-Beyerle, M.-E. Phonon Mode Transformation Across the Orthohombic-Tetragonal Phase Transition in a Lead Iodide Perovskite

DOI: 10.1021/acs.jpclett.8b02811
J. Phys. Chem. Lett. 2018, 9, 6853−6863

$CH_3NH_3PbI_3$: A Terahertz Time-Domain Spectroscopy Approach. *J. Phys. Chem. Lett.* **2016**, *7* (1), 1−6.
(12) Wright, A. D.; Verdi, C.; Milot, R. L.; Eperon, G. E.; Pérez-Osorio, M. A.; Snaith, H. J.; Giustino, F.; Johnston, M. B.; Herz, L. M. Electron-Phonon Coupling in Hybrid Lead Halide Perovskites. *Nat. Commun.* **2016**, *7*, 11755.
(13) Wasylishen, R.; Knop, O.; Macdonald, J. Cation Rotation in Methylammonium Lead Halides. *Solid State Commun.* **1985**, *56*, 581−582.
(14) Bakulin, A. A.; Selig, O.; Bakker, H. J.; Rezus, Y. L.; Müller, C.; Glaser, T.; Lovrincic, R.; Sun, Z.; Chen, Z.; Walsh, A.; Frost, J. M.; Jansen, T. L. C. Real-Time Observation of Organic Cation Reorientation in Methylammonium Lead Iodide Perovskites. *J. Phys. Chem. Lett.* **2015**, *6*, 3663−3669.
(15) Anusca, I.; Balciunas, S.; Gemeiner, P.; Svirskas, S.; Sanlialp, M.; Lackner, G.; Fettkenhauer, C.; Belovickis, J.; Samulionis, V.; Ivanov, M.; et al. Dielectric Response: Answer to Many Questions in the Methylammonium Lead Halide Solar Cell Absorbers. *Adv. Funct. Mater.* **2017**, *7*, 1700600.
(16) Onoda-Yamamuro, N.; Matsuo, T.; Suga, H. Dielectric Study of $CH_3NH_3PbX_3$ (X = Cl, Br, I). *J. Phys. Chem. Solids* **1992**, *53*, 935−939.
(17) Govinda, S.; Kore, B. P.; Bokdam, M.; Mahale, P.; Kumar, A.; Pal, S.; Bhattacharyya, B.; Lahnsteiner, J.; Kresse, G.; Franchini, C.; Pandey, A.; Sarma, D. D. Behavior of Methylammonium Dipoles in $MAPbX_3$ (X = Br and I). *J. Phys. Chem. Lett.* **2017**, *8*, 4113−4121.
(18) Lin, Q.; Armin, A.; Nagiri, R. C. R.; Burn, P. L.; Meredith, P. Electro-Optics of Perovskite Solar Cells. *Nat. Photonics* **2015**, *9*, 106−112.
(19) Juarez-Perez, A. J.; Sanchez, R. S.; Badia, L.; Garcia-Belmonte, G.; Kang, Y. S.; Mora-Sero, I.; Bisquert, J. Photoinduced giant dielectric constant in lead-halide perovskite solar cells. *J. Phys. Chem. Lett.* **2014**, *5*, 2390−2394.
(20) Sendner, M.; Nayak, P. K.; Egger, D. A.; Beck, S.; Müller, C.; Epding, B.; Kowalsky, W.; Kronik, L.; Snaith, H. J.; Pucci, A.; Lovrincic, R. Optical Phonons in Methylammonium Lead Halide Perovskites and Implications for Charge Transport. *Mater. Horiz.* **2016**, *3*, 613−620.
(21) Crothers, T. W.; Milot, R. L.; Patel, J. B.; Parrott, E. S.; Schlipf, J.; Müller-Buschbaum, P.; Johnston, M. B.; Herz, L. M. Photon Reabsorption Masks Intrinsic Bimolecular Charge-Carrier Recombination in $CH_3NH_3PbI_3$ Perovskite. *Nano Lett.* **2017**, *17*, 5782−5789.
(22) Valverde-Chavez, D. A.; Ponseca, C. S.; Stoumpos, C. C.; Yartsev, A.; Kanatzidis, M. G.; Sundström, V.; Cooke, D. G. Intrinsic Femtosecond Charge Generation Dynamics in Single Crystal $CH_3NH_3PbI_3$. *Energy Environ. Sci.* **2015**, *8*, 3700−3707.
(23) Hirasawa, M.; Ishihara, T.; Goto, T.; Uchida, K.; Miura, N. Magnetoabsorption of the Lowest Exciton in Perovskite-Type Compound $(CH_3NH_3)PbI_3$. *Phys. B* **1994**, *201*, 427−430.
(24) Poglitsch, A.; Weber, D. Dynamic disorder in Methylammoniumtrihalogenplumbates (II) Observed by Millimeter-Wave Spectroscopy. *J. Chem. Phys.* **1987**, *87*, 6373−6378.
(25) Löper, P.; Stuckelberger, M.; Niesen, B.; Werner, J.; Filipic, M.; Moon, S.-J.; Yum, J.-H.; Topic, M.; De Wolf, S.; Ballif, C. Complex Refractive Index Spectra of $CH_3NH_3PbI_3$ Perovskite Thin Films Determined by Spectroscopic Ellipsometry and Spectrophotometry. *J. Phys. Chem. Lett.* **2015**, *6*, 66−71.
(26) Jiang, Y.; Soufiani, A. M.; Gentle, A.; Huang, F.; Ho-Baillie, A.; Green, M. A. Temperature dependent optical properties of $CH_3NH_3PbI_3$ perovskite by spectroscopic ellipsometry. *Appl. Phys. Lett.* **2016**, *108*, 061905.
(27) Guerra, J. A.; Tejada, A.; Korte, L.; Kegelmann, L.; Töfflinger, J. A.; Albrecht, S.; Rech, B.; Weingärtner, R. Determination of the complex refractive index and optical bandgap of $CH_3NH_3PbI_3$ thin films. *J. Appl. Phys.* **2017**, *121*, 173104.
(28) Shirayama, M.; Kadowaki, H.; Miyadera, T.; Sugita, T.; Tamakoshi, M.; Kato, M.; Fujiseki, T.; Murata, D.; Hara, S.; Murakami, T. N.; et al. Optical Transitions in Hybrid Perovskite Solar Cells: Ellipsometry, Density Functional Theory, and Quantum Efficiency Analyses for $CH_3NH_3PbI_3$. *Phys. Rev. Appl.* **2016**, *5*, 014012.
(29) Leguy, A. M. A.; Azarhoosh, P.; Alonso, M. I.; Campoy-Quiles, M.; Weber, O. J.; Yao, J.; Bryant, D.; Weller, M. T.; Nelson, J.; Walsh, A.; et al. Experimental and theoretical optical properties of methylammonium lead halide perovskites. *Nanoscale* **2016**, *8*, 6317−6327.
(30) Ndione, P. F.; Li, Z.; Zhu, K. Effects of alloying on the optical properties of organicinorganic lead halide perovskite thin films. *J. Mater. Chem. C* **2016**, *4*, 7775−7782.
(31) Fox, M. *Optical Properties of Solids*, 2nd ed.; Oxford University Press, 2010.
(32) Frost, J. M.; Walsh, A. What Is Moving in Hybrid Halide Perovskite Solar Cells? *Acc. Chem. Res.* **2016**, *49*, 528−535.
(33) Brivio, F.; Walker, A.; Walsh, A. Structural and Electronic Properties of Hybrid Perovskites for High-Efficiency Thin-Film Photovoltaics from First-Principles. *APL Mater.* **2013**, *1*, 042111.
(34) Frost, J. M.; Butler, K. T.; Brivio, F.; Hendon, C. H.; van Schilfgaarde, M.; Walsh, A. Atomistic Origins of High-Performance in Hybrid Halide Perovskite Solar Cells. *Nano Lett.* **2014**, *14*, 2584−2590.
(35) Even, J.; Pedesseau, L.; Katan, C. Analysis of Multivalley and Multibandgap Absorption and Enhancement of Free Carriers Related to Exciton Screening in Hybrid Perovskites. *J. Phys. Chem. C* **2014**, *118*, 11566−11572.
(36) Miyata, K.; Zhu, X.-Y. Ferroelectric large polarons. *Nat. Mater.* **2018**, *17*, 379−381.
(37) Chen, T.; Foley, B. J.; Ipek, B.; Tyagi, M.; Copley, J. R. D.; Brown, C. M.; Choi, J. J.; Lee, S.-H. Rotational dynamics of organic cations in the $CH_3NH_3PbI_3$ perovskite. *Phys. Chem. Chem. Phys.* **2015**, *17*, 31278−31286.
(38) Leguy, A. M. A.; Frost, J. M.; McMahon, A. P.; Sakai, V. G.; Kockelmann, W.; Law, C.; Li, X.; Foglia, F.; Walsh, A.; O'Regan, B. C.; et al. The dynamics of methylammonium ions in hybrid organicinorganic perovskite solar cells. *Nat. Commun.* **2015**, *6*, 7124.
(39) Fabini, D. H.; Siaw, T. A.; Stoumpos, C. C.; Laurita, G.; Olds, D.; Page, K.; Hu, J. G.; Kanatzidis, M. G.; Han, S.; Seshadri, R. Universal Dynamics of Molecular Reorientation in Hybrid Lead Iodide Perovskites. *J. Am. Chem. Soc.* **2017**, *139*, 16875−16884.
(40) Beilsten-Edmands, J.; Eperon, G. E.; Johnson, R. D.; Snaith, H. J.; Radaelli, P. G. Non-Ferroelectric Nature of the Conductance Hysteresis in $CH_3NH_3PbI_3$ Perovskite-Based Photovoltaic Devices. *Appl. Phys. Lett.* **2015**, *106*, 173502.
(41) Eames, C.; Frost, J. M.; Barnes, P. R. F.; O'Regan, B. C.; Walsh, A.; Islam, M. S. Ionic Transport in Hybrid Lead Iodide Perovskite Solar Cells. *Nat. Commun.* **2015**, *6*, 7497.
(42) Klingshirn, C. F. *Semiconductor Optics*, 1st ed.; Springer, 1997; pp 165−166.
(43) Galkowski, K.; Mitioglu, A.; Miyata, A.; Plochocka, P.; Portugall, O.; Eperon, G. E.; Wang, J. T.-W.; Stergiopoulos, T.; Stranks, S. D.; Snaith, H. J.; Nicholas, R. J. Determination of the Exciton Binding Energy and Effective Masses for Methylammonium and Formamidinium Lead Tri-Halide Perovskite Semiconductors. *Energy Environ. Sci.* **2016**, *9*, 962−970.
(44) Miyata, A.; Mitioglu, A.; Plochocka, P.; Portugall, O.; Wang, J. T.-W.; Stranks, S. D.; Snaith, H. J.; Nicholas, R. J. Direct Measurement of the Exciton Binding Energy and Effective Masses for Charge Carriers in an Organic-Inorganic Tri-Halide Perovskite. *Nat. Phys.* **2015**, *11*, 582−587.
(45) Davies, C. L.; Filip, M. R.; Patel, J. B.; Crothers, T. W.; Verdi, C.; Wright, A. D.; Milot, R. L.; Giustino, F.; Johnston, M. B.; Herz, L. M. Bimolecular Recombination in Methylammonium Lead Triiodide Perovskite is an Inverse Absorption Process. *Nat. Commun.* **2018**, *9*, 293.
(46) Soufiani, A. M.; Huang, F.; Reece, P.; Sheng, R.; Ho-Baillie, A.; Green, M. A. Polaronic Exciton Binding Energy in Iodide and Bromide Organic-Inorganic Lead Halide Perovskites. *Appl. Phys. Lett.* **2015**, *107*, 231902.

DOI: 10.1021/acs.jpclett.8b02811
J. Phys. Chem. Lett. 2018, 9, 6853−6863

(47) Yamada, Y.; Nakamura, T.; Endo, M.; Wakamiya, A.; Kanemitsu, Y. Photoelectronic Responses in Solution-Processed Perovskite $CH_3NH_3PbI_3$ Solar Cells Studied by Photoluminescence and Photoabsorption Spectroscopy. *IEEE J. of Photovoltaics* **2015**, *5*, 401−405.
(48) Sestu, N.; Cadelano, M.; Sarritzu, V.; Chen, F.; Marongiu, D.; Piras, R.; Mainas, M.; Quochi, F.; Saba, M.; Mura, A.; Bongiovanni, G. Absorption F-Sum Rule for the Exciton Binding Energy in Methylammonium Lead Halide Perovskites. *J. Phys. Chem. Lett.* **2015**, *6*, 4566−4572.
(49) Yang, Y.; Ostrowski, D. P.; France, R. M.; Zhu, K.; van de Lagemaat, J.; Luther, J. M.; Beard, M. C. Observation of a Hot-Phonon Bottleneck in Lead-Iodide Perovskites. *Nat. Photonics* **2016**, *10*, 53−59.
(50) Menendez-Proupin, E.; Beltrán Ríos, C. L.; Wahnon, R. P. Nonhydrogenic Exciton Spectrum in Perovskite $CH_3NH_3PbI_3$. *Phys. Status Solidi RRL* **2015**, *9*, 559−563.
(51) Umari, P.; Mosconi, E.; De Angelis, F. Infrared Dielectric Screening Determines the Low Exciton Binding Energy of Metal-Halide Perovskites. *J. Phys. Chem. Lett.* **2018**, *9*, 620−627.
(52) Elliott, R. J. Intensity of Optical Absorption by Excitons. *Phys. Rev.* **1957**, *108*, 1384−1389.
(53) Milot, R. L.; Eperon, G. E.; Snaith, H. J.; Johnston, M. B.; Herz, L. M. Temperature-Dependent Charge-Carrier Dynamics in $CH_3NH_3PbI_3$. *Adv. Funct. Mater.* **2015**, *25*, 6218−6227.
(54) Davies, C. L.; Borchert, J.; Xia, C. Q.; Milot, R. L.; Kraus, H.; Johnston, M. B.; Herz, L. M. Impact of the Organic Cation on the Optoelectronic Properties of Formamidinium Lead Triiodide. *J. Phys. Chem. Lett.* **2018**, *9*, 4502−4511.
(55) Bokdam, M.; Sander, T.; Stroppa, A.; Picozzi, S.; Sarma, D. D.; Franchini, C.; Kresse, G. Role of Polar Phonons in the Photo Excited State of Metal Halide Perovskites. *Sci. Rep.* **2016**, *6*, 28618.
(56) Milot, R. L.; Klug, M. T.; Davies, C. L.; Wang, Z.; Kraus, H.; Snaith, H. J.; Johnston, M. B.; Herz, L. M. The Effects of Doping Density and Temperature on the Optoelectronic Properties of Formamidinium Tin Triiodide Thin Films. *Adv. Mater.* **2018**, *30*, 1804506.
(57) Amat, A.; Mosconi, E.; Ronca, E.; Quarti, C.; Umari, P.; Nazeeruddin, M. K.; Grätzel, M.; De Angelis, F. Cation-Induced Band-Gap Tuning in Organohalide Perovskites: Interplay of Spin-Orbit Coupling and Octahedra Tilting. *Nano Lett.* **2014**, *14*, 3608−3616.
(58) Grechko, M.; Bretschneider, S. A.; Vietze, L.; Kim, H.; Bonn, M. Vibrational Coupling between Organic and Inorganic SubLattices of Hybrid Perovskites. *Angew. Chem., Int. Ed.* **2018**, *57*, 13657−13661.
(59) Miyata, K.; Atallah, T. L.; Zhu, X.-Y. Lead halide perovskites: Crystal-liquid duality, phonon glass electron crystals, and large polaron formation Kiyoshi Miyata, Timothy. *Sci. Adv.* **2017**, *3*, e1701469.
(60) Zhu, X.; Su, H.; Marcus, R. A.; Michel-Beyerle, M. E. Computed and Experimental Absorption Spectra of the Perovskite $CH_3NH_3PbI_3$. *J. Phys. Chem. Lett.* **2014**, *5*, 3061−3065.
(61) Ahmed, T.; La-o-vorakiat, C.; Salim, T.; Lam, Y. M.; Chia, E. E. M.; Zhu, J.-X. Optical properties of organometallic perovskite: An ab initio study using relativistic GW correction and Bethe-Salpeter equation. *EPL* **2014**, *108*, 67015.
(62) Oga, H.; Saeki, A.; Ogomi, Y.; Hayase, S.; Seki, S. Improved Understanding of the Electronic and Energetic Landscapes of Perovskite Solar Cells: High Local Charge Carrier Mobility, Reduced Recombination, and Extremely Shallow Traps. *J. Am. Chem. Soc.* **2014**, *136*, 13818−13825.
(63) Savenije, T. J.; Ponseca, C. S.; Kunneman, L.; Abdellah, M.; Zheng, K.; Tian, Y.; Zhu, Q.; Canton, S. E.; Scheblykin, I. G.; Pullerits, T.; Yartsev, A.; Sundström, V. Thermally Activated Exciton Dissociation and Recombination Control the Carrier Dynamics in Organometal Halide Perovskite. *J. Phys. Chem. Lett.* **2014**, *5*, 2189−2194.
(64) Karakus, M.; Jensen, S. A.; D'Angelo, F.; Turchinovich, D.; Bonn, M.; Canovas, E. Phonon-Electron Scattering Limits Free Charge Mobility in Methylammonium Lead Iodide Perovskites. *J. Phys. Chem. Lett.* **2015**, *6*, 4991−4996.
(65) Shrestha, S.; Matt, G. J.; Osvet, A.; Niesner, D.; Hock, R.; Brabec, C. J. Assessing Temperature Dependence of Drift Mobility in Methylammonium Lead Iodide Perovskite Single Crystals. *J. Phys. Chem. C* **2018**, *122*, 5935−5939.
(66) Yi, H. T.; Wu, X.; Zhu, X.; Podzorov, V. Intrinsic Charge Transport across Phase Transitions in Hybrid OrganoInorganic Perovskites. *Adv. Mater.* **2016**, *28*, 6509−6514.
(67) Brenner, T. M.; Egger, D. A.; Rappe, A. M.; Kronik, L.; Hodes, G.; Cahen, D. Are Mobilities in Hybrid Organic-Inorganic Halide Perovskites Actually "High"? *J. Phys. Chem. Lett.* **2015**, *6*, 4754−4757.
(68) Even, J.; Paofai, S.; Bourges, P.; Letoublon, A.; Cordier, S.; Durand, O.; Katan, C. Carrier Scattering Processes and Low Energy Phonon Spectroscopy in Hybrid Perovskite Crystals. *Proc. SPIE* **2016**, *9743*, 97430M.
(69) Neukirch, A. J.; Nie, W.; Blancon, J.-S.; Appavoo, K.; Tsai, H.; Sfeir, M. Y.; Katan, C.; Pedesseau, L.; Even, J.; Crochet, J. J.; Gupta, G.; Mohite, A. D.; Tretiak, S. Polaron Stabilization by Cooperative Lattice Distortion and Cation Rotations in Hybrid Perovskite Materials. *Nano Lett.* **2016**, *16*, 3809−3816.
(70) Yu, P. Y.; Cardona, M. *Fundamentals of Semiconductors*, 1st ed.; Springer, 1996.
(71) Fröhlich, H. Electrons in Lattice Fields. *Adv. Phys.* **1954**, *3*, 325−361.
(72) Feynman, R. P. Slow Electrons in a Polar Crystal. *Phys. Rev.* **1955**, *97*, 660−665.
(73) Biaggio, I.; Hellwarth, R. W.; Partanen, J. P. Band Mobility of Photoexcited Electroncs in $Bi_{12}SiO_{20}$. *Phys. Rev. Lett.* **1997**, *78*, 891−894.
(74) He, Y.; Galli, G. Perovskites for Solar Thermoelectric Applications: A First Principle Study of $CH_3NH_3AI_3$ (A = Pb and Sn). *Chem. Mater.* **2014**, *26*, 5394−5400.
(75) Wang, Y.; Zhang, Y.; Zhang, P.; Zhang, W. High Intrinsic Carrier Mobility and Photon Absorption in the Perovskite $CH_3NH_3PbI_3$. *Phys. Chem. Chem. Phys.* **2015**, *17*, 11516−11520.
(76) Filippetti, A.; Mattoni, A.; Caddeo, C.; Saba, M. I.; Delugas, P. Low Electron-Polar Optical Phonon Scattering as a Fundamental Aspect of Carrier Mobility in Methylammonium Lead Halide $CH_3NH_3PbI_3$ Perovskites. *Phys. Chem. Chem. Phys.* **2016**, *18*, 15352−15362.
(77) Yu, Z.-G. Rashba Effect and Carrier Mobility in Hybrid Organic-Inorganic Perovskites. *J. Phys. Chem. Lett.* **2016**, *7*, 3078−3083.
(78) Frost, J. M. Polaron Mobility in Halide Perovskites. *Phys. Rev. B: Condens. Matter Mater. Phys.* **2017**, *96*, 195202.
(79) Hellwarth, R. W.; Biaggio, I. Mobility of an Electron in a Multimode Polar Lattice. *Phys. Rev. B: Condens. Matter Mater. Phys.* **1999**, *60*, 299−307.
(80) Menendez-Proupin, E.; Palacios, P.; Wahnon, P.; Conesa, J. C. Self-Consistent Relativistic Band Structure of the $CH_3NH_3PbI_3$ Perovskite. *Phys. Rev. B: Condens. Matter Mater. Phys.* **2014**, *90*, 045207.
(81) Umari, P.; Mosconi, E.; De Angelis, F. Relativistic GW calculations on $CH_3NH_3PbI_3$ and $CH_3NH_3SnI_3$ Perovskites for Solar Cell Applications. *Sci. Rep.* **2015**, *4*, 4467.
(82) Madelung, O., Ed. *Semiconductors − Basic Data*, 2nd ed.; Springer: Berlin, 1996.
(83) Rehman, W.; Milot, R. L.; Eperon, G. E.; Wehrenfennig, C.; Boland, J. L.; Snaith, H. J.; Johnston, M. B.; Herz, L. M. Charge-Carrier Dynamics and Mobilities in Formamidinium Lead Mixed-Halide Perovskites. *Adv. Mater.* **2015**, *27*, 7938−7944.
(84) Rehman, W.; McMeekin, D. P.; Patel, J. B.; Milot, R. L.; Johnston, M. B.; Snaith, H. J.; Herz, L. M. Photovoltaic Mixed-Cation Lead Mixed-Halide Perovskites: Links Between Crystallinity, Photo-Stability and Electronic Properties. *Energy Environ. Sci.* **2017**, *10*, 361−369.
(85) Egger, D. A.; Bera, A.; Cahen, D.; Hodes, G.; Kirchartz, T.; Kronik, L.; Lovrincic, R.; Rappe, A. M.; Reichman, D. R.; Yaffe, O.

DOI: 10.1021/acs.jpclett.8b02811
J. Phys. Chem. Lett. 2018, 9, 6853−6863

What Remains Unexplained about the Properties of Halide Perovskites? *Adv. Mater.* **2018**, *30*, 1800691.
(86) Rakita, Y.; Cohen, S. R.; Kedem, N. K.; Hodes, G.; Cahen, D. Mechanical properties of $APbX_3$ (A = Cs or CH_3NH_3; X = I or Br) perovskite single crystals. *MRS Commun.* **2015**, *5*, 623−629.
(87) Yaffe, O.; Guo, Y.; Tan, L. Z.; Egger, D. A.; Hull, T.; Stoumpos, C. C.; Zheng, F.; Heinz, T. F.; Kronik, L.; Kanatzidis, M. G.; et al. Local Polar Fluctuations in Lead Halide Perovskite Crystals. *Phys. Rev. Lett.* **2017**, *118*, 136001.
(88) Bonn, M.; Miyata, K.; Hendry, E.; Zhu, X.-Y. Role of Dielectric Drag in Polaron Mobility in Lead Halide Perovskites. *ACS Energy Lett.* **2017**, *2*, 2555−2562.
(89) Dastidar, S.; Li, S.; Smolin, S. Y.; Baxter, J. B.; Fafarman, A. T. Slow Electron-Hole Recombination in Lead Iodide Perovskites Does Not Require a Molecular Dipole. *ACS Energy Lett.* **2017**, *2*, 2239−2244.
(90) Zhu, H.; Trinh, M. T.; Wang, J.; Fu, Y.; Joshi, P. P.; Miyata, K.; Jin, S.; Zhu, X.-Y. Organic Cations Might Not Be Essential to the Remarkable Properties of Band Edge Carriers in Lead Halide Perovskites. *Adv. Mater.* **2017**, *29*, 1603072.
(91) Kulbak, M.; Cahen, D.; Hodes, G. How Important is the Organic Part of Lead Halide Perovskite Photovoltaic Cells? Efficient $CsPbBr_3$ Cells. *J. Phys. Chem. Lett.* **2015**, *6*, 2452−2456.
(92) Zhang, M.; Zhang, X.; Huang, L.-Y.; Lin, H.-Q.; Lu, G. Charge Transport in Hybrid Halide Perovskites. *Phys. Rev. B: Condens. Matter Mater. Phys.* **2017**, *96*, 195203.
(93) Wehrenfennig, C.; Liu, M.; Snaith, H. J.; Johnston, M. B.; Herz, L. M. Charge Carrier Recombination Channels in the Low-Temperature Phase of Organic-Inorganic Lead Halide Perovskite Thin Films. *APL Mater.* **2014**, *2*, 081513.
(94) Hrostowski, H.; Morin, F. J.; Geballe, T.; Wheatley, G. H. Hall Effect and Conductivity of InSb. *Phys. Rev.* **1955**, *100*, 1672−1676.
(95) Stillman, G. E.; Wolfe, C. M.; Dimmock, J. O. Hall Coefficient Factor for Polar Mode Scattering in n-Type GaAs. *J. Phys. Chem. Solids* **1970**, *31*, 1199−1204.
(96) Godinho, N.; Brunnschweiler, A. Epitaxial Indium Arsenide by Vacuum Evaporation. *Solid-State Electron.* **1970**, *13*, 47−52.
(97) Glisksman, M.; Weiser, K. Electon Mobility in InP. *J. Electrochem. Soc.* **1958**, *105*, 728−731.
(98) Rode, D. L. Electron Transport in InSb, InAs, and InP. *Phys. Rev. B* **1971**, *3*, 3287−3299.
(99) Kumar, M. H.; Dharani, S.; Leong, W. L.; Boix, P. P.; Prabhakar, R. R.; Baikie, T.; Shi, C.; Ding, H.; Ramesh, R.; Asta, M.; Grätzel, M.; Mhaisalkar, S. G.; Mathews, N. Lead-Free Halide Perovskite Solar Cells with High Photocurrents Realized Through Vacancy Modulation. *Adv. Mater.* **2014**, *26*, 7122−7127.
(100) Parrott, E. S.; Green, T.; Milot, R. L.; Johnston, M. B.; Snaith, H. J.; Herz, L. M. Interplay of Structural and Optoelectronic Properties in Formamidinium Mixed TinLead Triiodide Perovskites. *Adv. Funct. Mater.* **2018**, *28*, 1802803.
(101) Parrott, E. S.; Milot, R. L.; Stergiopoulos, T.; Snaith, H. J.; Johnston, M. B.; Herz, L. M. Effect of Structural Phase Transition on Charge-Carrier Lifetimes and Defects in $CH_3NH_3SnI_3$ Perovskite. *J. Phys. Chem. Lett.* **2016**, *7*, 1321−1326.
(102) Milot, R. L.; Eperon, G. E.; Green, T.; Snaith, H. J.; Johnston, M. B.; Herz, L. M. Radiative Monomolecular Recombination Boosts Amplified Spontaneous Emission in $HC(NH_2)_2SnI_3$ Perovskite Films. *J. Phys. Chem. Lett.* **2016**, *7*, 4178−4184.

DOI: 10.1021/acs.jpclett.8b02811
J. Phys. Chem. Lett. 2018, 9, 6853−6863